A New Family of Transition Metal Nitrides

R. Yu and X.-F. Zhang

Materials Sciences Division, Lawrence Berkeley National Laboratory, Berkeley, CA94720, USA.

Transition metal nitrides are of great interest in both fundamental science and technical applications[1-7]. Most of early transition metal nitrides are well known hard materials or superconductors. In contrast, not much success has been achieved in exploration of the late transition metal nitrides, especially for the platinum group and noble metals[8-10]. Very recently, a significant progress in this direction has been made: Platinum nitride, the first binary metal nitride in the platinum group was synthesized under high pressures and temperatures[11]. Here we report the theoretical investigations of a new family of transition metal nitrides. Using *ab initio* calculations of the mechanical stability, we show that the platinum nitride is stable with a fluorite type structure, but not with the reported zinc-blende structure[11], and the properties calculated based on the fluorite structure agreed well with experimental data[11]. Staying with the fluorite structure, we extended the calculations to the nitrides of the whole platinum group and noble metals and found another three mechanically stable phases, i.e., AgN_2, AuN_2 and IrN_2. Our calculations predict a high possibility for synthesizing a new family of metal nitrides.

The zinc-blende and the fluorite structures have face-centred-cubic unit cells, with a space group of $F\bar{4}3m$ and Fm3m, respectively[12] (Fig. 1). In each unit cell there are four metal atoms and eight tetrahedral interstitial sites in the metal sublattice. The zinc-blende nitride phase is formed when half number of the tetrahedral sites are occupied by N atoms as shown in Fig. 1a, therefore the zinc-blende structure is quite open. When all

of the tetrahedral sites are occupied by N atoms, the fluorite phase is formed, Fig. 1b. So the chemical formula for the zinc-blende phase is MN, but MN_2 for the fluorite phase, here M denotes transition metal elements.

In our computations, the lattice constants (a) and the bulk moduli (B) were evaluated from the Birch-Murnaghan[13] fit to the total energies as a function of the unit cell volume. The calculation results are listed in Table 1. The calculations for elemental Pt were also performed for comparison. For Pt, the calculated average values (a=3.928 Å, B=279 GPa) match the experimental ones (a=3.924 Å, B=276 GPa)[12,14] very well. The lattice constants for both PtN and PtN_2 are sufficiently close to the experimentally determined ones. The calculated lattice constant for PtN_2 is 3.7% larger than that for PtN. Apparently, filling four more N atoms in the tetrahedral sites does not result in a considerable expansion of the unit cell. The experimental bulk modulus[11] is significantly larger than the calculated values for PtN and PtN_2. The reason will be discussed later in this letter.

The mechanical stability of a crystal means that the strain energy must be positive. For a cubic crystal, it implies the following restrictions[15]: $c_{44} > 0$, $c_{11} > |c_{12}|$, and $c_{11} + 2c_{12} > 0$, where c_{11}, c_{12}, and c_{44} are the elastic stiffness constants. In the present work, the elastic stiffness constants were calculated by computing the total energies of the strained crystals, and fitting them to the third-order polynomial of strains. Since there are three independent elastic constants for a cubic phase[15], three types of strain, i.e., the volume change, and volume-conserved tetragonal and rhombohedral shear strains, were applied to the optimized structures to calculate the elastic constants.

The total energy as a function of the tetragonal distortion for the zinc-blende PtN and fluorite PtN_2 are shown in Figs. 2a and 2b, respectively. The polynomial fit to Fig. 2a gives the shear modulus of $c' = (c_{11}-c_{12})/2 = -17$ GPa for PtN. It means that the zinc-

blende PtN is not mechanically stable; the cubic lattice would distort spontaneously to a tetragonal lattice to lower the energy. Fig. 2b shows that the fluorite structured PtN_2 has positive moduli with the tetragonal distortion and in fact to all the distortions as demonstrated in our calculations, therefore the structure is mechanically stable. The elastic stiffness constants c_{ij}, polycrystalline shear modulus G, Young's modulus E, and Poisson's ratio v were calculated and the results are listed in Table 2. The polycrystalline shear modulus of G = 127 GPa, calculated from the single crystal elastic constants based on the Voigt-Reuss-Hill[16] averaging scheme, is about two times higher than the value for the elemental Pt (61 GPa)[14]. From the correlation between the hardness and the shear modulus[17-18], it is expected that the platinum nitride is much harder than Pt. Considering that the density of the platinum nitride is only half of that of the platinum, the enhancement in hardness is quite remarkable.

We also calculated the X-ray diffraction patterns (not shown here) for the zinc-blende and the fluorite platinum nitrides and found no noticeable difference. This was in expectation because the two structures have the same Pt sublattice, and the scattering from these heavy metal atoms dominates the X-ray diffraction intensities.

The stoichiometric PtN_2 contains 67 at% N. However, in ref. 11, the measured N composition was about 50 at%. The difference suggests a nitrogen deficiency in the synthesized phase, like in many anion-deficient fluorite structured fast-ion conductors[19], such as CeO_2 and ZrO_2. The experimentally determined lattice constant, which is 2.2% smaller than the calculated value, may be attributed to the existence of the nitrogen vacancies. The existence of the vacancies also explains the difference between the measured and the calculated bulk moduli. As seen in Table 1, the measured bulk modulus[11] is about 28% greater than the calculated value for PtN_2. Experimentally, the bulk modulus was derived from the pressure increase with volume contraction[11]. In experiments, nitrogen was used as the pressure medium, nitrogen atoms which were

pressed into the nitrogen-deficient lattice under pressure should compensate the volume contraction, resulting in an increased bulk modulus value. Such a process also implies fast nitrogen diffusion in PtN_2, just as high oxygen mobility in the fast-ion conductors such as CeO_2 and ZrO_2.

The chemical bonding and electronic structure were analysed for PtN_2. The band structure and density of states (DOS) at zero pressure are shown in Fig. 3a and 3b, respectively. No energy gap is seen, indicating a metallic nature of the platinum nitride. There is a deep minimum in DOS where the Fermi level locates, giving the DOS at the Fermi level ($N(E_F)$) of only 0.35 states/eV unit cell. Such a DOS distribution is a typical stability effect by formation of a pseudogap[20-21], where the decrease of total DOS at the Fermi level is accompanied by shifting the occupied bonding states to lower energies and the unoccupied antibonding states to higher energies. The low $N(E_F)$ actually indicates that the platinum nitride is a poor metal, in agreement with the experimental observations[11]. The states between -18 eV and -13 eV are mainly composed of N(2s) states. The states above -8 eV are mainly composed of Pt(5d) states (t_{2g} and e_g) and N(2p) states. Due to the stronger Pt(t_{2g})-N(2p) interactions, the t_{2g} band has a larger dispersion than that of the e_g band, with the antibonding part almost empty.

The similar chemical properties of the noble and platinum group metals suggest a high possibility for formation of other stable transition metal nitrides with the fluorite structure in additional to PtN_2. Mechanical stabilities of MN_2, where M = Ru, Rh, Pd, Ag, Os, Ir, Pt and Au, were computed. As a consequence, another three stable nitrides were identified, they were AgN_2, AuN_2 and IrN_2, and the calculated elastic constants are shown in Table 3.

In conclusion, a new family of late transition metal nitrides is predicted from theoretical computations. Four nitrides, PtN_2, AgN_2, AuN_2, and IrN_2, were concluded to

be mechanically stable with the fluorite structure. Among the four, platinum nitride has just been reported recently to be synthesized under high pressures and temperatures, and the phase sustained in ambient conditions. It is highly expectable that other nitrides predicted in the present work can also be synthesized in forms of bulk or thin film under suitable conditions. The new materials will stimulate a series of experimental and theoretical research efforts in exploring their physical, chemical, and mechanical properties.

Methods

The full-potential linearized augmented plane waves (LAPW) method[22-23] was employed in this study. This method is one of the most accurate schemes in solving the Kohn-Sham equations in density-functional theory[24-25]. Augmented plane wave plus local orbitals (APW+lo)[26-27] were used for valence states, and LAPW for other states. A fully relativistic calculation was performed for core states, whereas the valence states were treated in a scalar relativistic scheme. The total and partial densities of states (DOS) were obtained using a modified tetrahedron method of Blöchl *et al*.[28] The total Brillouin zones were sampled with 5000 k points. Both the local density approximation (LDA)[29] and the generalized gradient approximation (GGA)[30] exchange correlation functional were employed in the present calculations. Since it is known that the LDA usually underestimates the lattice constants and overestimates the elastic constants, whereas the GGA overestimates the lattice constants and underestimates the elastic constants, we used the arithmetic average of the LDA and the GGA values as the theoretical value.

1. Toth, L. E. *Transition metal carbides and nitrides* (Academic Press, New York, 1971).

2. Pierson, H. *Handbook of Refractory Carbides and Nitrides: Properties, Characteristics and Applications* (Noyes Publications, Westwood, New Jersey, 1996).

3. Jhi, S.-H., Ihm, J., Louie, S. G. & Cohen, M. L. Electronic mechanism of hardness enhancement in transition-metal carbonitrides. *Nature* **399**, 132-134 (1999).

4. McMillan, P. F. New materials from high-pressure experiments. *Nature Mater*. **1**, 19-25 (2003).

5. Yamanaka, S., Hotehama, K. & Kawaji, H. Superconductivity at 25.5 K in electron-doped layered hafnium nitride. *Nature* **392**, 580-582(1998).

6. Zerr, A., Miehe, G. & Boehler, R. Synthesis of cubic zirconium and hafnium nitrides having Th_3P_4 structure. *Nature Mater*. **2**, 185-189 (2003).

7. Kroll, P. Hafnium nitride with thorium phosphide structure: physical properties and an assessment of the Hf-N, Zr-N, and Ti-N phase diagrams at high pressures and temperatures. *Phys. Rev. Lett.* **90**, 125501 (2003).

8. Maruyama, T. & Morishita T. Copper nitride and tin nitride thin films for write-once optical recording media. *Appl. Phys. Lett.* **69**, 890-891 (1996).

9. Shanley, E. S. & Ennis J. L. The chemistry and free energy of formation of silver nitride. *Ind. Eng. Chem. Res.* **30**, 2503-2506 (1991).

10. Krishnamurthy, S. et al. Nitrogen ion irradiation of Au(110): Photoemission spectroscopy and possible crystal structures of gold nitride. *Phys. Rev. B* **70**, 045414 (2004).

11. Gregoryanz, E. *et al.* Synthesis and characterization of a binary noble metal nitride. *Nature Mater.* **3**, 294-297 (2004).

12. Pearson, W. B. *A Handbook of Lattice Spacings and Structures of Metals and Alloys* (Pergamon Press, New York, 1958).

13. Birch, F. Finite strain isotherm and velocities for single-crystal and polycrystalline NaCl at high pressures and 300 K. *Journal of Geophysical Research* **95**, 1257-1268 (1978).

14. Brandes, E. A. *Smithells Metal Reference Book* 6th ed. (Butterworth, London, 1983).

15. Nye, J. F. *Physical Properties of Crystals* (Oxford University Press, Oxford, 1985).

16. Hill, R. The elastic behaviour of a crystalline aggregate. *Proc. Phys. Soc. London* **65**, 349-354 (1952).

17. Teter, D. M. Computational alchemy: the search for new superhard materials. *Mater. Res. Soc. Bull.* **23**, 22-27 (1998).

18. Brazhkin, V. V., Lyapin, A. G. & Hemley, R. J. Harder than diamond: dreams and reality. *Phil. Mag. A* **82**, 231-253 (2002).

19. Boivin, J.C. & Mairesse, G. Recent material developments in fast oxide ion conductors. *Chem. Mater.* **10**, 2870-2888 (1998).

20. Hoffmann, R. *Solids and Surfaces* (VCH Publishers, New York, 1988).

21. Carlsson, A. E. & Meschter, P. J. in *Intermetallic Compounds: Vol. 1* (eds Westbrook J. H. & and Fleischer R. L.) 55-76 (Wiley, Chichester, 1994).

22. Singh, D. J. *Planewaves, Pseudopotentials and the LAPW Method* (Kluwer Academic, Boston, 1994).

23. Blaha, P., Schwarz, K., Madsen, G. K. H., Kvasnicka, D. & Luitz, J. *WIEN2k, An Augmented Plane Wave + Local Orbitals Program for Calculating Crystal Properties* (Karlheinz Schwarz, Techn. Universität Wien, Austria), 2001. ISBN 3-9501031-1-2.

24. Hohenberg, P. & Kohn, W. Inhomogeneous electron gas. *Phys. Rev.* **136**, B864-B871 (1964).

25. Kohn, W. & Sham, L. J. Self-consistent equations including exchange and correlation effects. *Phys. Rev.* **140**, A1133-A1138 (1965).

26. Sjöstedt, E., Nordström, L. & Singh, D. J. *Solid State Commun.* **114**, 15-20 (2000).

27. Madsen, G. K. H., Blaha, P., Schwarz, K., Sjöstedt, E., & Nordström, L., *Phys. Rev. B* **64**, 195134 (2001).

28. Blöchl, P., Jepsen, O. & Andersen, O. K. *Phys. Rev. B* **49**, 16223-16233 (1994).

29. Perdew, J. P. & Wang, Y. *Phys. Rev. B* **45**, 13244-13249 (1992).

30. Perdew, J. P., Burke, K. & Ernzerhof, M. *Phys. Rev. Lett.* **77**, 3865-3868 (1996).

This work was partly supported by the Laboratory Directed Research and Development Program of Lawrence Berkeley National Laboratory under the Department of Energy Contract No. DE-AC03-76SF00098.

Correspondence and requests for materials should be addressed to R.Y. (e-mail: ryu@lbl.gov).

Figure Legends:

Figure 1 The unit cell schematics. a, Zinc-blende structure; b, Fluorite structure. The large and small spheres represent metal and N atoms, respectively.

Figure 2 The total energies of platinum nitrides as a function of the tetragonal distortion. a, Zinc-blende phase; b, Fluorite phase. The zinc-blende phase is not stable to the tetragonal distortion, while the fluorite phase is.

Figure 3 Electronic structure of PtN_2. a. Band structure; b, Total density of states (DOS). The Fermi level lies at the energy zero. The low DOS at the Fermi level indicates that PtN_2 is a poor metal.

Table 1. The lattice constants and bulk moduli of platinum nitrides and platinum.

	Platinum nitrides			Pt	
	exp.	zinc-blende PtN (cal)	fluorite PtN_2 (cal)	experimental	calculation
a (Å)	4.804	4.736	4.912	3.924	3.928
		4.692 (LDA)	4.866 (LDA)		3.890 (LDA)
		4.780 (GGA)	4.958 (GGA)		3.967 (GGA)
B (GPa)	372	219	290	276	279
		244 (LDA)	316 (LDA)		320 (LDA)
		194 (GGA)	264 (GGA)		238 (GGA)

LDA: local density approximation. GGA: generalized gradient approximation.

Table 2. The elastic constants of PtN_2.

	c_{11}	c_{12}	c_{44}	G	E	v
LDA	532	208	122	137	359	0.32
GGA	457	167	99	116	303	0.31
Average	495	188	111	127	332	0.31

LDA**:** local density approximation**.** GGA**:** generalized gradient approximation. All elastic constants are in GPa, except the dimensionless Poisson's ratio v.

Table 3. The calculated lattice parameters and elastic constants of AgN_2, AuN_2 and IrN_2.

		a (Å)	c_{11}	c_{12}	c_{44}	B	G	E	v
AgN_2	LDA	5.013	268	189	57	215	50	138	0.40
	GGA	5.141	215	138	59	164	50	136	0.37
	Average	5.077	242	164	58	190	50	137	0.39
AuN_2	LDA	5.035	371	183	71	246	80	216	0.36
	GGA	5.144	316	139	52	198	65	175	0.36
	Average	5.090	344	161	62	222	73	197	0.36
IrN_2	LDA	4.801	464	339	124	381	95	262	0.39
	GGA	4.882	391	273	115	313	88	242	0.38
	Average	4.842	428	306	120	347	92	253	0.38

LDA**:** local density approximation**.** GGA**:** generalized gradient approximation. All elastic constants are in GPa, except the dimensionless Poisson's ratio v.

a

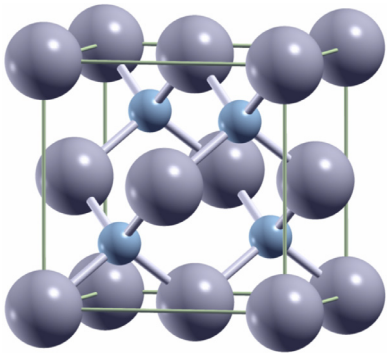

b

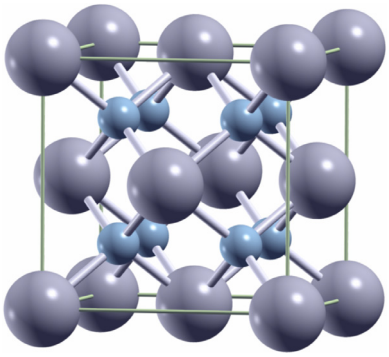

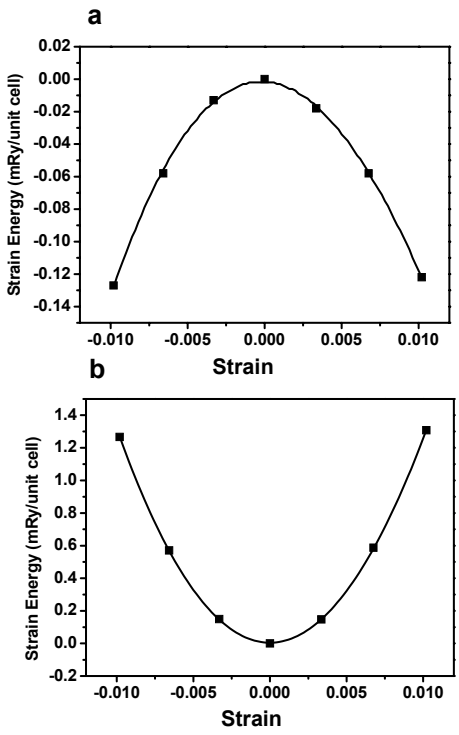
a
Strain Energy (mRy/unit cell)
0.02
0.00
-0.02
-0.04
-0.06
-0.08
-0.10
-0.12
-0.14
-0.010
-0.005
0.000
0.005
0.010
Strain
b
Strain Energy (mRy/unit cell)
1.4
1.2
1.0
0.8
0.6
0.4
0.2
0.0
-0.2
-0.010
-0.005
0.000
0.005
0.010
Strain

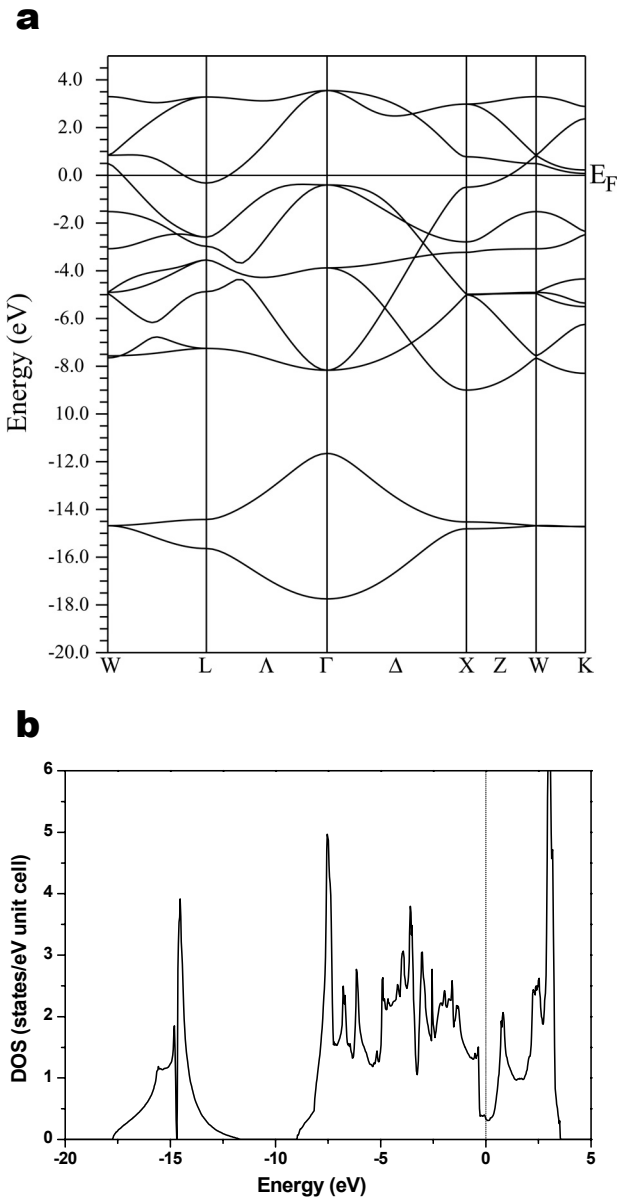
a
4.0
2.0
0.0
-2.0
-4.0
-6.0
-8.0
10.0
-12.0
-14.0
-16.0
-18.0
-20.0
Energy (eV)
E_F
W
L
Λ
Γ
Δ
X
Z
W
K
b
DOS (states/eV unit cell)
Energy (eV)